



EFFECTS OF AMORPHOUS NANO-SILICA ADDITIONS ON MECHANICAL AND DURABILITY PERFORMANCE OF SCC MIXTURES

George Quercia^{1,2}, Przemek Spiesz², Götz Hüsken³ and Jos Brouwers²

¹Materials innovation institute (M2i), Delft, The Netherlands

²Eindhoven University of Technology, Eindhoven, The Netherlands

³BAM Federal Institute for Materials Research and Testing, Berlin, Germany

ABSTRACT

In the recent years the application of nanotechnology in building materials has increased exponentially. One of the most referred and used nano-materials is amorphous silica with particles size in the nano-range, even though its application and effect in concrete has not been fully understood yet. It has been reported that nano-silica (nS) addition increases the compressive strength and reduces the overall permeability of hardened concrete due to the pozzolanic properties which are resulting in finer hydrated phases (C-S-H gel) and densified microstructure (nano-filler and anti leaching effects). These effects enhance the durability of concrete structures such as bridges, quays or off-shore oil facilities in marine environments.

In this study two different types of nano-silica were applied in self-compacting concrete (SCC), both having similar particle size distributions (PSD) but produced in two different processes (fumed powder silica and precipitated silica in colloidal suspension). The influence of nano-silica on SCC was investigated with respect to the properties of concrete in the fresh state (workability) and hardened state (mechanical properties and durability). Additionally, the densification of microstructure of the hardened concrete was verified by SEM and EDS analyses. The obtained results demonstrate that an efficient use of nano-silica in SCC can improve its mechanical properties and durability. Considering the reactivity of the two nano-silica studied, colloidal type shown more reactivity at early age, which influenced all the final SCC properties.

Keywords: Nano-silica, Concrete, Self Compacting, Durability, Chloride and Freeze-thaw.

INTRODUCTION

Nowadays the micro-level does not provide enough insights into building materials. Therefore, all around the world, increasing amounts of research funding are being diverted into the nano-level, which is claimed to have tremendous potential for the future [1]. The fundamental processes that govern the properties of concrete are affected by the performance of the material on a nanoscale. The main hydration product of cement-based materials, the C-S-H gel, is a natural nano-structured material [1-4]. The mechanical properties and the durability of concrete mainly depend on the gradual refining microstructure of the hardened cement paste and the gradually improving of the paste-aggregate interface zone (ITZ) [5].

One of the most referred to and used new cementitious nano-materials is amorphous silica with a particle size in the nano-range, even though its application and effect in concrete has not been fully understood yet. It has been reported that nano-silica addition increases the compressive strength and reduces the overall permeability of hardened concrete due to the pozzolanic properties, which are resulting in finer hydrated phases (C-S-H gel) and densified microstructure (nano-filler and anti-Ca(OH)₂-leaching effects) [5-20]. These effects may enhance the durability of concrete elements and structures. There are different commercial types of nano-silica additives available on the market, which are produced in different ways such as precipitation, pyrolysis, sol-gel and others [19]. The main characteristic of nano-silica, such as particle size distribution, specific density, specific surface area, pore structure, and reactivity (surface silanol groups), depends on the production method [17]. Despite the existence of several studies that describe the main properties and characteristics of concrete with nano-silica particles, most of them focus on the applications of nano-silica as an anti-bleeding [20-26] and as a compressive strength enhancement additive [12][13][25-29]. Furthermore, durability and sustainability of concrete infrastructures is becoming of critical importance for the construction industry. In this context, SCC is a type of concrete that has generated tremendous interest since its initial development in Japan by Okamura [30]. SSC was developed to reach durable concrete structures. The aim was to develop a concrete with a high flowability and high resistance to segregation, which also could be cast on-site without compaction. The high flowability is obtained by the use of a new generation superplasticizers, high amounts of fine particles and in some cases a viscosity modifying agent (added to reduce segregation and bleeding). Due to the presence of a high number of fines, the pore structure of SCC differs from the pore structure of traditional concrete. According to Audenaert et al. [31] the actual application of SCC might be somewhat risky due to the lack of knowledge concerning the actual durability of this new material. In the literature only a few reports on the effects of nano-silica additions on the durability of SCC are available [25][27][29]. In addition, the difference in the reactivity of nano-silica due to its production route has not been reported yet.

In this study two different types of nano-silica were applied in SCC, both having similar particle size distribution (PSD) but produced in two different processes (fumed powder silica and precipitated silica in colloidal suspension). The influence of the nano-silica on the SCC was investigated with respect to the properties of concrete in the fresh state (workability) and in the hardened state (mechanical properties and durability). Additionally, the densification of microstructure of the hardened concrete was analysed by SEM and EDS techniques.

MATERIALS AND METHODS

Materials and SCC mix design

The Portland cement used was CEM I 42.5N (ENCI, Netherlands), as classified by [32]. This cement consists of at least 95% of Portland cement clinker; the initial setting time is 60 min, the water demand of 38.9% by weight, and the compressive strength of 21 ± 3 N/mm² for 2 days and 51 ± 4 N/mm² at 28 days [32]. The coarse aggregates used were composed of broken granite in fractions 8-16 mm and 2-8 mm. Two different sands were used: drained river sand (0-4 mm) and microsand (Granite Import B.V., Belgium), composed mainly of natural sandstone waste (0-1 mm) generated in crushing process. Ground limestone powder provided by Omya Belgium (Betocarb® MQ) was applied as the filler. Two different commercial nS additives were selected to produce two different SCC batches: one colloidal nano-silica suspension from Akzo Nobel Germany (Cembinder® 8) and one fumed or pyrolytic powder nano-silica provided by Elkem Materials Norway (Submicron silica 995). Both nS have a similar PSD and specific surface areas measured by BET (Brunauer-Emmet-Teller method [33]), following the standard DIN-ISO 9277-2005 [34]. Furthermore, one superplasticizer (SP) of the 3rd generation, based on polycarboxylate ethers (Glenium® 51, BASF Netherlands) was added in order to adjust the

workability of the mix. A summary of the general characteristics of all materials used is shown in Table 1 and their PSDs are depicted in Figure 1.

Table 1 – Properties of used materials

| Materials | Specific density [g/cm ³] | BET [m ² /g] | pH | Solid content [% w/w] | Loss of ignition [L.O.I] | Computed SSA [m ² /m ³] |
|-----------------------|---------------------------------------|-------------------------|------|-----------------------|--------------------------|--|
| CEM I 42.5N | 3.14 | 1 | - | - | 2.8 | 1,699,093 |
| Colloidal nano-silica | 1.40 | 50 | 9.5 | 50 | - | 46,110,081 |
| Powder nano-silica | 2.15 | 56 | 5.0* | - | 0.5 | 48,175,461 |
| Limestone powder | 2.71 | - | - | - | - | 1,234,362 |
| Microsand (sandstone) | 2.64 | - | - | - | - | 193,514 |
| Sand 0-4 | 2.64 | - | - | - | - | 14,251 |
| Granite 2-8 | 2.65 | - | - | - | - | 1,740 |
| Granite 8-16 | 2.65 | - | - | - | - | 515 |
| Superplasticizer | 1.10 | - | 7.0 | 35 | - | - |

(*) 4% w/w in water

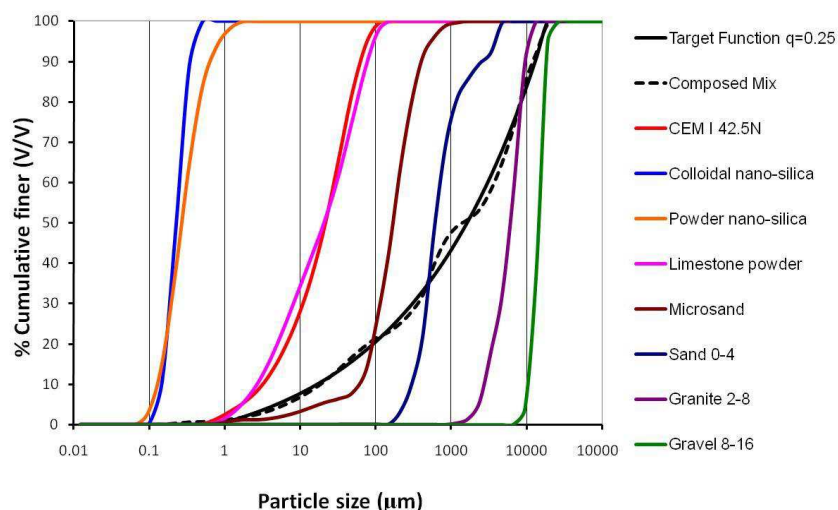


Figure 1 – PSD of materials used and mix design target function based on [36]

For the composition of SCC mixes, the mix design concept described in [35] was used. This design concept makes use of an optimization algorithm described in [36] in order to compose the mix proportions between all the solid ingredients of the concrete mix, following the theory of continuously graded granular mixtures with a geometric particle size distribution (“target function”). In the mix design optimization process the distribution modulus (q) of 0.25 was selected, together with the following constrains: cement content of 340 kg/m³, w/c ratio 0.45 and air content in the fresh mix of 1% by vol. The cement content and the w/c ratio were selected based on NEN-EN 206-1 (2008) [37] for XS3 exposure classes (aggressive exposure to chlorides originating from seawater). In addition, a flow class of fresh concrete F7 (630-800 mm) was selected as target, taking into consideration the Dutch recommendation BRL 1801 [38] for SCC. An example of the target curve and the composed SCC mix grading curve is shown in Figure 1. The final mix proportioning and characteristic of one reference mix without nano-silica and two mixes with nS additions are presented in Table 2.

Table 2 – Composition and characteristics of the designed SCC mixes

| Materials | Reference | Colloidal nano-silica [kg/m ³] | Powder nano-silica |
|--|-----------|--|-----------------------|
| CEMI 42.5N | 340.0 | 340.0 | 340.1 |
| Nano-silica | 0.0 | 12.8 | 12.8 |
| Limestone powder | 179.4 | 151.8 | 151.9 |
| Microsand (sandstone) | 125.0 | 141.3 | 141.4 |
| Sand 0-4 | 624.3 | 617.9 | 618.0 |
| Granite 2-8 | 733.8 | 735.6 | 735.7 |
| Granite 8-16 | 274.7 | 274.2 | 274.3 |
| Water | 153.0 | 153.0 | 153.0 |
| SP | 3.4 | 6.5 | 6.5 |
| Air [% V] | 1.0 | 1.0 | 1.0 |
| Density [g/cm ³] | 2.427 | 2.427 | 2.430 |
| w/c | 0.45 | 0.45 | 0.45 |
| w/p | 0.267 | 0.270 | 0.270 |
| Powder content [l/m ³] | 194.2 | 192.7 | 192.6 |
| Composed surface [m ² /m ³] | 277,972 | 547,905 | 554,428 |
| SP content [g/m ²] | 0.0122 | 0.0119 | 0.0117 |
| SP content [% bwoc] | 1.0 | 1.9 | 1.9 |

bwoc: Based on the weight of cement

Test methods

Fresh concrete properties

Using the provided materials, three SCC mixes (2 batches for each mix) were prepared according to the mix proportions listed in Table 2. These SCCs were mixed for five minutes in a compulsory mixer and subsequently tested for their fresh concrete properties according to the procedure recommended by EFNARC committee [39]. The following parameters were determined: V-funnel time, slump flow, fresh concrete density, packing fraction and air content. An overview of the fresh concrete properties of the tested mixes is given in Table 3.

Table 3 – Fresh concrete properties of prepared SCC mixes

| Value | Reference | Colloidal nano-silica | Powder nano-silica |
|------------------------------------|-----------|--------------------------|-----------------------|
| Slump flow [mm] | 690 - 720 | 664 - 701 | 685 - 720 |
| V-Funnel time [s] | 35.0 | 20.5 | 24.5 |
| Fresh density [g/cm ³] | 2.399 | 2.384 | 2.392 |
| Air content [%V]* | 1.15 | 1.79 | 1.58 |
| Packing density [%]* | 83.55 | 82.91 | 83.12 |

* Calculated value

Hardened concrete: mechanical properties

To test the properties of hardened concrete, 38 cubes (150 mm) were cast of each mix, cured sealed during the first day, stripped from the mould after 24 hours and cured subsequently in water until their test age was reached, according to the prescribed storing conditions given by BS-EN 12390-2 [40]. The compressive strength was determined after 1, 3, 7, 28 and 91 days on 3 cubes for each mix. The compressive strength test was performed according to BS-EN 12390-3 [41]. In addition, the splitting tensile strength was determined after 28 days on 3 cubes, following the procedure given in BS-EN 12390-6 [42].

Hardened concrete: durability tests

a) Permeable (water accessible) porosity

The permeable porosity affects the transport properties and durability of concrete. It is related to many deterioration processes driven by the transport properties of concrete [43]. In this context, six concrete discs (height of approx. 15 mm, diameter of 100 mm) for each SCC mixes were extracted from the inner layers of six different cubes. In total 18 discs were used to calculate the permeable porosity, following the modified procedure described in the ASTM 1202 [44]. The vacuum-saturation technique was applied in order to fill the accessible pores with water as this technique is referred as the most efficient by Safiuddin and Heran [43].

b) Penetration of water under pressure

The depth of penetration of water under pressure was tested according to BS-EN 12390-8 [45] after 28 days. The samples (standard cubes, 3 cubes for SCC reference and 2 for each SCC mixes with nano-silica) were exposed to water under pressure (5 bars) for 72 hours and subsequently split in order to determine the maximum depth of the water penetration.

c) Rapid Chloride Migration test (RCM) and conductivity test

The Rapid Chloride Migration test (performed according to NT Build 492 [46]) is a commonly used accelerated technique for determination of the chloride transport rate in concrete. The output value of the test – the chloride migration coefficient D_{RCM} – is employed in the service life design codes (DuraCrete [47], CUR Durability Guideline [48]) for concrete elements and structures exposed to chlorides.

Concrete cores (diameter of 100 mm) were extracted from three cubes of each concrete mix. Two specimens for the RCM test (cylinders, diameter of 100 mm and height of 50 mm) were retrieved from each cube, which gives six specimens per one concrete mix (three for 28 days tests and three for 90 days tests). The RCM test was performed according to NT Build 492 [46]. One day before the RCM test the specimens were pre-conditioned and eventually tested at the age of 28 and 90 days. The duration of the test for all the samples lasted 24 hours. For each concrete mix three concrete specimens were tested. After the test the penetration of chlorides was measured and the values D_{RCM} were calculated.

Besides the RCM test, the electrical resistance was measured by using the so-called ‘two electrodes’ method [49]. For this, an AC test signal ($f = 1$ kHz) was applied between two stainless-steel electrodes and the resistance of the concrete sample placed between the electrodes was registered. Finally, the conductivity of the samples was calculated taking into account their thickness and transversal area.

d) Chloride diffusion test

Because the nano-silica additions change the ionic strength, the pH and the conductivity of the pore solution [50], the results obtained using the RCM test may be influenced, as the procedure of this test [51] is based only on experience with OPC systems. On the contrary, the natural diffusion tests are only affected by the pore structure (permeability and tortuosity), chloride binding and by the chloride concentration gradient. Thus, the chloride diffusion test should be more reliable for SCC with nano-silica additions than the RCM test.

Three specimens for the diffusion test (cylinders, diameter of 100 mm and height of 50 mm) were extracted from the cubes of each prepared concrete mix. Diffusion tests were carried out at the age of 28 days following the procedure described in NT Build 443 [51]. All faces of the specimens were coated with epoxy resin except for one face, left uncovered in order to allow the

chloride to penetrate the samples just from one surface. The specimens were immersed in chloride solution with concentration of 165 g/l for 63 days at room temperature in sealed and de-aired container. After the exposure period, the concrete specimens were ground in layers by using the Profile Grinder 1100 (German Instruments). The grinding was performed on the area of 73 mm in diameter. Exact grinding depth increments are adjustable, between 0.5 mm and 2.0 mm. The produced powder was collected for the determination of the total chloride concentration profile, following the procedure described by [52]. The obtained chloride concentration profiles were fit to the solution of the Fick's second law, in order to obtain the apparent chloride diffusion coefficient (D_{app}) and the chloride concentration in the surface layer of concrete.

e) Freeze-thaw resistance (surface scaling test)

As a further durability assessment, the freeze-thaw test were performed on SCC samples, even though their air content in the fresh mix was less than the recommended value of 4% volume [37]. The freeze-thaw resistance, expressed by the scaling factor (S_n), was determined following NEN-EN 12390-9 [53]. However, the test samples were different from the ones specified in the standard – concrete cylinders (height of 50 mm and diameter of 100 mm) were used instead of slabs. The samples were sealed in tight rubber sleeves and placed in PU insulation of 10 mm thickness. Three specimens were tested per each mix. The samples were cut from a cast cube after 14 days and sealed after 25 days. Subsequently, the samples were surface saturated with demineralised water for 3 days until the age of 28 days. After the saturation, the demineralised water was replaced by a 3% by mass NaCl solution and the freeze-thaw cycles were started. The applied temperature profile was oriented on the recommendations given in NEN-EN 12390-9 [53]. In total, 56 freeze-thaw cycles were performed. The surface scaling was measured after 7, 14, 28, 42 and 56 cycles.

Microstructural characterization and analysis

The morphology of the prepared concrete was analyzed with a high resolution scanning electron microscope (FEI Quanta 600 FEG-SEM) using a Schottky field emitter gun (at voltage of 10 keV and 0.6 mbar of low-vacuum pressure). Furthermore, a general chemical analysis was performed using EDAX energy dispersive spectroscopy (EDS) in a low vacuum mode.

RESULTS AND DISCUSSION

Fresh concrete properties

The properties of concrete in the fresh state are presented in Table 3. All three mixes fulfill the requirements for the flow class type F7 (630 to 800 mm), specified in BRL 1801 [38]. Only the mix with colloidal nano-silica resulted in a flow nearby the lower limit of this target range. Another interesting finding is that the SP requirement to fulfill the same flow class for the prepared mixes was relative constant with an average value of 0.0119 g/m². This suggests that it is possible to calculate the required amount of SP if the composed surface of all the solid ingredients in concrete is known. Another implication of this result is that the SP requirement is more related to the changes in the internal surface area of the mix than to the concentration (by mass) of the nano-silica addition, as was previously reported by Sobolev et al. [17]. In that study it was concluded that 0.21% of additional SP is needed for each 1% of nano-silica added to a standard concrete composition.

Considering the V-funnel time, only the two mixes with nano-silica fulfill the requirements on the viscosity class VF2 (funnel time range 9 - 25 s), established by the European guidelines on SCC [39]. Although the reference mix does not fulfill the viscosity class, it is in the range as

proposed by Hunger (2010) [35] for high powder content SCC mixes. In addition, no segregation or blocking was observed for any mixes. A high V-funnel time was already reported as a typical behavior of SCC with an increased concentration of limestone powder [54-56]. As also can be seen in Table 4, the mixes with nano-silica have higher air content compared to the reference mix, which is caused by the higher viscosity of the paste due to application of particles with high specific surface area (SSA). The air entrainment was also confirmed by the difference between the designed and the measured density of concrete (Table 3 and 4).

Hardened concrete: mechanical properties

Compressive strength

The 1 day compressive strength of the reference mix was higher than the strength of mixes with nano-silica (Figure 2a). At this age the mix with powder type nano-silica showed the lowest compressive strength. This behavior can be related to the difference in the reactivity of both nano-silica samples. The colloidal nano-silica is synthesized at low temperature and has a higher concentration of silanol groups on its surface. During the development of the strength over time, the mix with colloidal nano-silica showed the highest compressive strength from 3 until 91 days of aging. An interesting observation is that at 7 days the mix with powder nano-silica starts to present similar compressive strength than the reference mix, as the result of increasing pozzolanic reaction with the $\text{Ca}(\text{OH})_2$ generated during the OPC hydration. At 91 days, the powder nano-silica developed higher compressive strength than reference SCC. In case of the SCC with colloidal nano-silica the 91 days compressive strength was almost the same as 28 days, mainly because this type of silica is more reactive, so it was consumed faster at early ages.

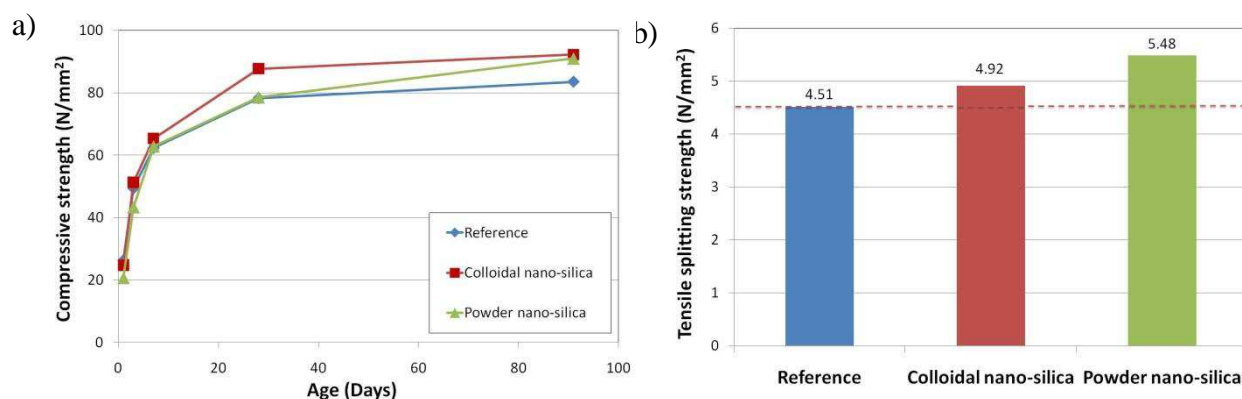


Figure 2 – Mechanical properties of the tested SCC mixes,
a) Compressive strength development and b) 28 days splitting tensile strength

Tensile splitting strength

The determined average 28 days tensile splitting strength of the reference mix was 4.51 N/mm^2 . The equivalent values for the mixes with colloidal and powder nano-silica additives are higher and amount to 4.92 N/mm^2 and 5.48 N/mm^2 respectively (Figure 2b). A possible explanation for the higher splitting tensile strength of the samples containing nano-silica is given by the strongest bond between the hardened paste and the aggregates. Nano-silica improved the quality of the interfacial zone (ITZ) due to the precipitation of smaller and stronger (high stiffness) C-S-H gel and the accelerated the rate of hydration, as was reported for several researchers [5-21]. Further analysis will be presented in microstructural analysis section.

Hardened concrete: durability

Permeable porosity

The results of the measurements of the permeable porosity of the SCC mixes are presented in Figure 3a. These results show that the SCC reference mix has slightly lower porosity (12.1%) than the mixes with the two types of nano-silica additions (12.5%). The porosity and the tortuosity of pores in hardened cement pastes are normally reduced when pozzolanic material is added, and this influences many properties such as the compressive and splitting tensile strength [57]. Nevertheless, Yogendran and Langan [58] stated that for micro-silica additions the total pore volume is not necessarily changed, but larger pores appear to be subdivided into smaller pores. Apparently, the same behaviour was found for SCC with nano-silica additions. The air content in the fresh mix probably influenced the final porosity; some researchers [43] state that the vacuum saturation technique is able to take into account these pores as well. This means that the porosity values shown in Fig. 3a considered also differences in the air content of the mixes (the lowest the air content the lowest the permeable porosity). Taking into account the error of the porosity measurement technique (12.3 to 56.0 %), the three SCC mixes studied had a very similar water permeable porosity.

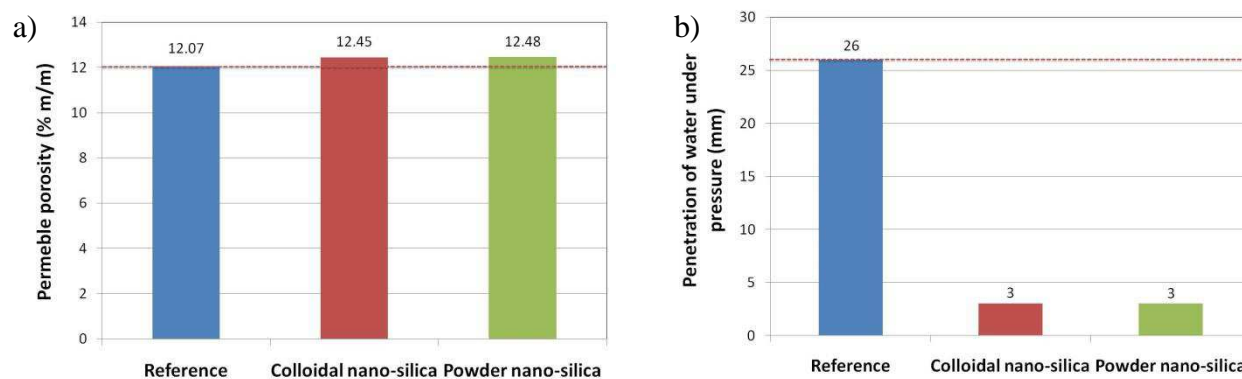


Figure 3 – 28 days results of the tested SCC mixes, a) water permeable or accessible porosity, b) maximum depth of penetration of water under pressure.

Penetration of water under pressure

The test results of the penetration of water under pressure are shown in Figure 3b. According to [27], all tested samples are in low permeability range (less than 30 mm of penetration depth). Additionally, the two SCC with both types of nano-silica presented penetration depth lower than 5 mm. This implies that the addition of 3.8% nano-silica results in concrete which is almost impermeable to water. Similar permeability improvements were reported by Raïess-Ghasemi et al. [27] for conventional concrete with micro and nano-silica additions. The results also suggest that despite the similar permeable porosity of all SCC mixes, the nano-silica samples have very low effective water permeability (less interconnected pores and/or finer pore structure). A similar phenomenon was already reported by Yogendran and Langan [58] for HPC with micro-silica additions, where the total porosity was not affected, but the permeability was decreased in one order of magnitude.

Conductivity

Figure 4a shows the average values of conductivity, measured on cylindrical SCC samples extracted from the cubes, Its is clearly shown that the conductivity of the SCC with nano-silica addition is reduced by more than 50% compared to the SCC reference mix. Meanwhile, the SCC with colloidal nano-silica presented a slightly lower conductivity than samples with powder

nano-silica. This behaviour is an indication of the ability of the water-saturated pore structure of concrete to transport electrical charge. Different authors [59][60] established that the conductivity is directly related to the porosity, the pore structure (tortuosity, connectivity and conductivity) and to the pH values of the pore solutions (pH value is lower in presence of nano-silica). In general, higher porosity means higher conductivity due the presence of more volumetric fractions of pores. The lower conductivity values shown by the SCC with nano-silica is the result of the pore structure refinement (less connected pores) due to the progressive pozzolanic reaction and higher hydration degree (see the microstructural analysis section). The small difference between the two types of silica is mainly related with higher reactivity of the colloidal nano-silica, which promotes a more compact and finer microstructure (higher stiffness C-S-H gel) than the powder nano-silica. Nevertheless, the values are in line with results of the water pressure penetration test and with determined compressive strengths. Conductivity can also be related with the compressive strength as was demonstrated by Andrade et al. [61].

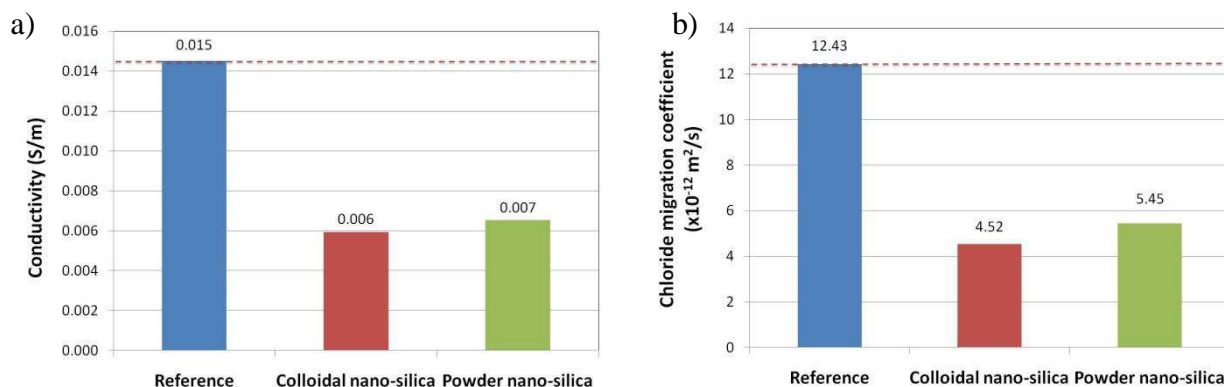


Figure 4 – 28 days results of the tested SCC mixes, a) conductivity, b) chloride migration coefficient (D_{RCM}).

Rapid chloride migration test (RCM)

Figure 4b presents the average values of calculated chloride migration coefficients (D_{RCM}) of each SCC mixes studied. Like the conductivity test results, the migration coefficients are much lower for the mixes containing nano-silica. In this context, the SCC mix with colloidal nano-silica shows the best performance. The explanations of this behavior are the same as previously discusses for the conductivity test results. A finer porosity, greater tortuosity and more precipitated C-S-H gel decrease the mobility of the chloride ions into the SCC pore solution.

The output value of the RCM test can be employed in service life design codes [47][48] for concrete elements and structures exposed to chlorides. When comparing all the obtained D_{RCM} values with the values suggested in CUR Durability Guideline [48] for 100 years of service life, the SCC reference mix is out of the range of the designed exposure class XS3. On the contrary both SCC mixes with nano-silica addition satisfied the exposure class XS3 with a concrete cover depth of 50 mm. On the other hand, comparing the obtained D_{RCM} values to similar SCC mixes published in literature, the values obtained for the reference mix are in line with SCC mix having high amount of limestone powder (between 8 and $12 \times 10^{-12} \text{ m}^2/\text{s}$ at 28 days [31]), meanwhile the values obtained for the SCC mixes with nano-silica additions showed similar reported value of SCC composed of slag cement or fly ash additions with similar w/b ratio and cement content (between 4 and $5 \times 10^{-12} \text{ m}^2/\text{s}$ [31]).

Chloride diffusion test

In Figure 5a the obtained apparent chloride diffusion coefficients (D_{app}) of the three SCC mixes are shown. A trend similar to the D_{RCM} was obtained for the diffusion test. The largest D_{app} was computed for the reference SCC ($9.61 \times 10^{-12} \text{ m}^2/\text{s}$). Both SCC with nano-silica additions showed

D_{app} of $4.45 \times 10^{-12} \text{ m}^2/\text{s}$ and $3.55 \times 10^{-12} \text{ m}^2/\text{s}$ for powder nano-silica and for colloidal nano-silica, respectively. Even though the changes of the chemical balance of the pore solution due to the additions of nano-silica, the D_{app} found are in the same order of magnitude that the D_{RCM} .

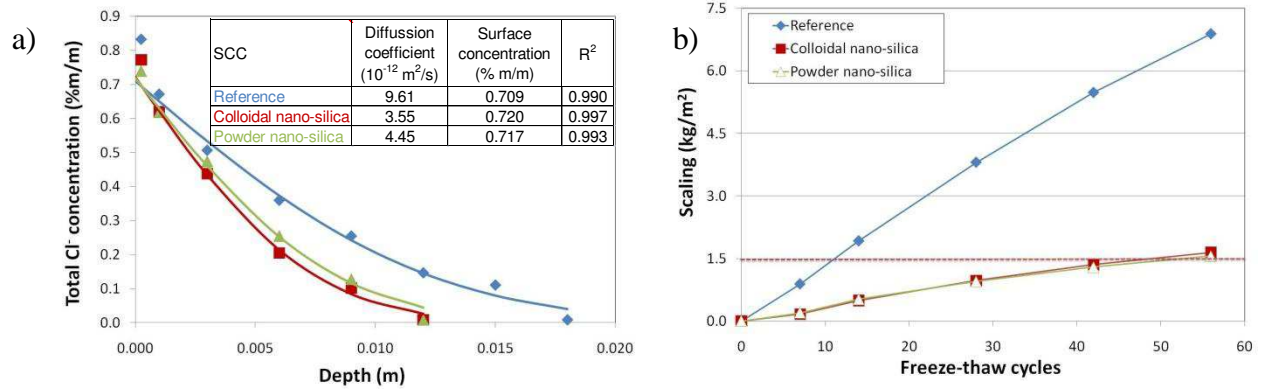


Figure 5 – a) Chloride diffusion profiles of the tested SCC mixes, b) cumulative scaling factor after 56 freeze-thaw cycles (3% NaCl solution).

Freeze-thaw resistance

The results of the freeze-thaw scaling test of the three selected SCC mixes are shown in Figure 5b. The failure of SCC reference mix, taking into account the maximum scaling value of 1.5 kg/m^2 at 28 cycles recommended in [62], occurred about the 11th cycle. In contrast, the SCC mixes with nano-silica additions show scaling factor lower than the referred limit for non-air entrained concrete until 28 cycles. These SCC mixes failed after 48 cycles. Similar to the other properties determined, the SCC with colloidal nano-silica additions showed a better behavior than the SCC with powder nano-silica. The freeze-thaw resistance depends on the compressive strength, porosity, air content and others parameters such as the air-bubbles spacing and pore sizes [63]. Better resistance to the freeze-thaw cycles of the SCC with nano-silica additions can be attributed to its denser and more compacted microstructure. The highly stiff C-S-H gel and the refined pore structure results in a limited intrusion of water and in an improved resistance to changes of temperature in the concrete surface. Despite the better freeze-thaw resistance of the SCC with nano-silica compared to the reference mix, its scaling values are larger than the recommended values of 0.5 kg/m^2 after 56 cycles, suggested by Stark and Wicht [64] for a concrete classified as having good resistance against freeze-thaw exposure. Nevertheless, with an air entrainment admixture that guarantees a minimum air content of 4%, the freeze-thaw resistance of SCC with nano-silica could be a promising mix with high resistance to the freeze-thaw exposure.

Concrete microstructural characterization analysis

All SCC mixes were analysed in a low vacuum environment (0.6 mbar) using FEG-SEM device. The objective of this analysis was to support the findings shown in the present research. In this context, in Figure 6 some morphological characteristics of the microstructure of the SCC reference mix are presented. SCC reference mix has a dense structure and relative good ITZ (Figure 6a). Nevertheless, its microstructure is heterogeneous, with high amounts of small pores and big size C-S-H gel structures present. Additionally, acicular (rod like) structures (Figure 6b) were identified, typically found in high concentration limestone powder concrete and possibly formed of Ettringite needles and AFt phases that are reach in CO_3^{2-} . The formation of rod like AFt phases in cement pastes with high calcium carbonate concentration was observed by [65]. In addition, well crystallized hexagonal Portlandite ($\text{Ca}(\text{OH})_2$) plates were clearly precipitated in the cement matrix and in the largest air pores (Figure 6c). Normally, the presence of high amounts of $\text{Ca}(\text{OH})_2$ results in a lower chloride intrusion resistance and lower compressive

strength. These findings are in line with the mechanical and durability test results discussed previously.

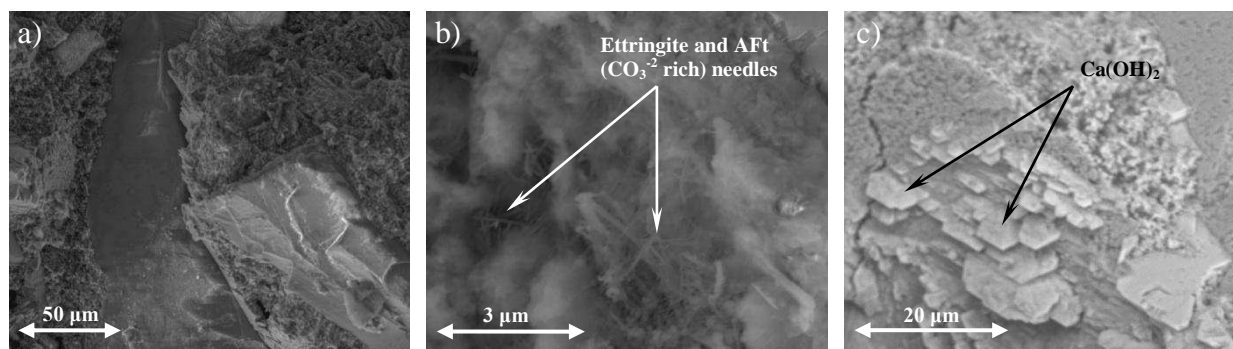


Figure 6 – Microstructure low vacuum (0.6 mbar) FEG-SEM photomicrographs of **SCC reference mix**, a) cement matrix and aggregate ITZ, b) rod like calcium carboaluminate hydrate or Ettringite needle and c) precipitated hexagonal Portlandite plate crystals.

As can be observed in Fig. 7a, the SCC with colloidal nano-silica additions shows a more homogeneous microstructure compared to the reference mix. This microstructure is characterized by compact and small sizes of C-S-H gel morphology. As a consequence, a better ITZ was also confirmed by SEM (Figure 7c). It is important to notice that neither rod nor needle type precipitates nor well precipitated $\text{Ca}(\text{OH})_2$ crystals were found in the microstructural analysis. This confirms that the additions of nano-silica causes a refinement of the microstructure and induces precipitation of small and high stiffness sized C-S-H gel. The improvement of the microstructure was also reflected in the mechanical properties (compressive and splitting strength) due to the fact that the pozzolanic gel structure present better mechanical properties than the C-S-H gel precipitated in standard OPC concrete [19]. In addition, the resistance to the chloride intrusion was enhanced because of the densification of the microstructure and the high specific surface area of the gel [50]. The high reactivity of the colloidal nano-silica SCC was also confirmed in Figure 7b, where a small C-S-H gel precipitates were observed around limestone powder and agglomerates of nano-particles.

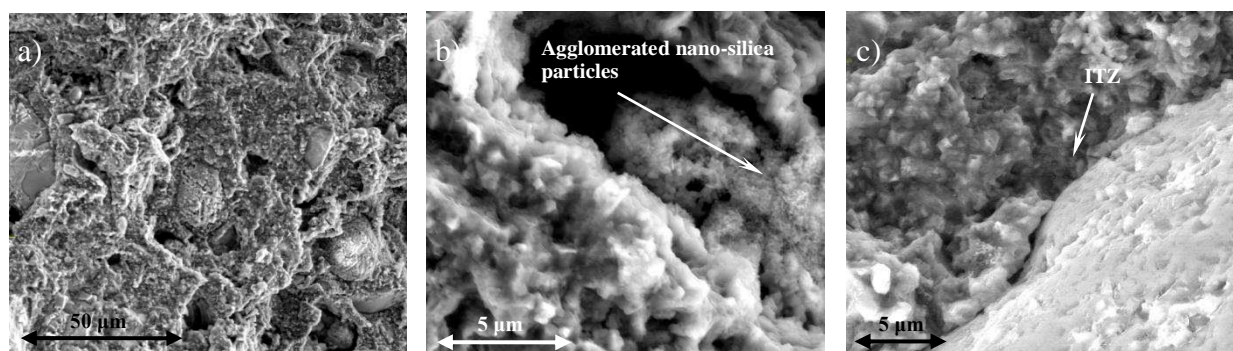


Figure 7 – Microstructure low vacuum (0.6 mbar) FEG-SEM photomicrographs of **SCC colloidal nano-silica mix**, a) cement matrix, b) agglomerates in a pore and c) aggregate dense ITZ.

Also in the case of SCC with powder nano-silica, a similar microstructural analysis was performed. Its microstructure is found to be refined (Figure 8a) but not as much as with the colloidal nano-silica. Apparently, due the fact that this nano-silica was produced at high temperature (more compact, lower concentration of silanol groups) its pozzolanic reactivity is lower than the colloidal one. Nevertheless, a relatively homogeneous matrix was observed with more small pores distributed in it (Figure 8b). Even though the microstructure was refined due to the addition of the powder silica nano-particles, it was still possible to observe remnant rod like or needles of AFt phases in the matrix (Figure 8c).

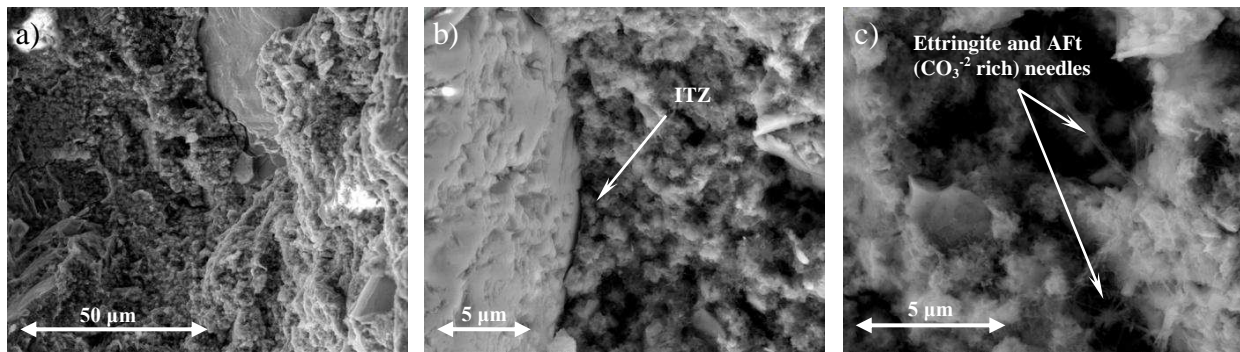


Figure 8 – Microstructure low vacuum (0.6 mbar) FEG-SEM photomicrographs of **SCC powder nano-silica mix**, a) cement matrix, b) aggregates ITZ and c) rod like precipitates.

The difference in observed microstructures can explain the results obtained for the two SCC with both types of nano-silica additions, where SCC with the colloidal nano-silica presented better results in all performed tests. The SCC with colloidal nano-silica presented a denser paste matrix and a better aggregates ITZ than the SCC with powder nano-silica. In addition, a refined microstructure was obtained (no Ettringite needles were found or identified). These refined were translated in better mechanical and durability properties of the SCC tested. Despite the lower reactivity at early ages of the powder nano-silica, the properties of the SCC were still significantly improved compared to the reference mix. However, the spherical shape and the lower reactivity of the powder nano-silica favoured to a better fresh behaviour of the SCC when it is compared with the colloidal nano-silica SCC mix.

CONCLUSIONS

Based on the results of the performed experiments on the design of SCC mixes with two types of nano-silica additions and their effect on the mechanical and durability properties, the following conclusions can be drawn:

- The results of the fresh state behaviour of SCC demonstrated that concrete with addition of 3.8% of nano-silica (based on the mass of cement) shows similar flowing and viscosity behaviour as the reference mix without nano-silica. Small differences in the reactivity at early age were also confirmed for both types of nano-silica studied. The difference in reactivity produces the increased air content in the mix due to a higher internal viscosity of the paste.
- The compressive and tensile splitting strengths of SCC were improved by the addition of both types of nano-silica. The highest compressive strength was found for the colloidal nano-silica SCC, meanwhile the highest splitting tensile strength was found for the powder type nano-silica SCC.
- The water permeable porosity of the three SCC mixes showed similar behaviour. On the contrary, when nano-silica is added, the SCC mixes become almost impermeable to the penetration of water under pressure.
- All durability indicators of the SCC studied (conductivity, chloride migration, chloride diffusion, and freeze-thaw resistance) were improved with the additions of 3.8% of both types of the nano-silica. Moreover, the SCC with colloidal nano-silica showed slightly better properties than the SCC with powder nano-silica additions.
- The microstructural analysis of the hardened SCC reveals that the additions of nano-silica particles produced a homogeneous microstructure, characterized by compact and small sized C-S-H gel. As a consequence, a denser ITZ was produced. The additions of nano-silica caused a refinement of the microstructures (less interconnected pore structure) and induced precipitation of small sizes C-S-H gel having high stiffness. The

improvement of the microstructure was reflected by the mechanical properties (compressive and splitting tensile strength) due to the fact that the pozzolanic gel structure presents better mechanical properties than the C-S-H gel precipitated in standard OPC concrete. In addition, the resistance against chloride intrusion was enhanced because of the microstructure densification effect. The high reactivity and faster pozzolanic behaviour of the colloidal nano-silica particles at early ages produced a more refined microstructure than the SCC with powder nano-silica.

ACKNOWLEDGEMENTS

This research was carried out under project number M81.1.09338 in the framework of the Research Program of the Materials innovation institute M2i and The European Community's Seventh Framework Programme, ProMine: Nano-particle products from new mineral resources in Europe, FP7-NMP-2008-LARGE-2 under grant agreement 228559. The authors also wish to express their gratitude to following sponsors of the Building Materials research group at TU Eindhoven: Bouwdienst Rijkswaterstaat, Graniet-Import Benelux, Kijlstra Betonmortel, Struyk Verwo, Attero, Enci, Provincie Overijssel, Rijkswaterstaat Directie Zeeland, A&G Maasvlakte, BTE, Alvon Bouwsystemen, V.d. Bosch Beton, Selor, Twee "R" Recycling, GMB, Schenk Concrete Consultancy, Intron, Geochem Research, Icopal, BN International, APP All Remove, Consensor, Eltomation, Knauf Gips, Hess ACC Systems and Kronos (chronological order of joining).

REFERENCES

1. Scrivener, K.L. and Kirkpatrick, R.J. "Innovation in use and research on cementitious material", *Cement and Concrete Research* 38 (2008), pp. 128-136.
2. Sanchez, F. and Sobolev, K. "Nanotechnology in concrete – A review", *Construction and Building Materials* 24 (2010), pp. 2060-2071.
3. Constantinides, G. and Ulm, F. "The nanogranular nature of C–S–H", *Journal of the Mechanics and Physics of Solids* 55 (2007), pp. 64-90.
4. Richarson, I.G. "The nature of the hydration products in hardened cement pastes", *Cement and Concrete Composites* 22 (2000), pp. 97-113.
5. Nili, M., Ehsani, A. and Shabani, K. "Influence of nano-SiO₂ and micro-silica on concrete performance", *Proceedings Second International Conference on Sustainable Construction Materials and Technologies*. June 28-30 (2010). Universita Ploitecnica delle Marche, Ancona, Italy, 2010.
6. Qing, Y., Zenan, Z., Deyu, K. and Rongshen, Ch. "Influence of nano-SiO₂ addition on properties of hardened cement paste as compared with silica fume", *Construction and Building Materials* 21 (2007), pp. 539–545.
7. Senff, L., Labrincha, J.A., Ferreira, V.M., Hotza, D. and Repette, W.L. "Effect of nano-silica on rheology and fresh properties of cement pastes and mortars", *Construction and Building Materials* 23 (2009), pp. 2487–2491.
8. Lin, K.L., Chang, W.C., Lin, D.F., Luo, H.L. and Tsai, M.C. "Effects of nano-SiO₂ and different ash particle sizes on sludge ash–cement mortar", *Journal of Environmental Management* 88 (2008), pp. 708-714.
9. Bjornstrom, J., Martinelli, A, Matic, A., Borjesson, L. and Panas, I. "Accelerating effects of colloidal nano-silica for beneficial calcium–silicate–hydrate formation in cement", *Chemical Physics Letters* 392 (2004), pp. 242-248.
10. Senff, L., Hotza, D., Repette, W.L., Ferreira, V.M. and Labrincha, J.A. "Mortars with nano-SiO₂ and micro-SiO₂ investigated by experimental design", *Construction and Building Materials* 24 (8) (2010), pp. 1432-1437.
11. Ji, T. "Preliminary study on the water permeability and microstructure of concrete incorporating nano-SiO₂", *Cement and Concrete Research* 35 (2005), pp. 1943-1947.
12. Li, G. "Properties of high-volume fly ash concrete incorporating nano-SiO₂", *Cement and Concrete Research* 34 (2004), pp. 1043-1049.
13. Gaitero, J.J., Campillo, I. and Guerrero, A. "Reduction of the calcium leaching rate of cement paste by addition of silica nanoparticles", *Cement and Concrete Research* 38 (2008), pp. 1112-1118.
14. Green, B.H. "Development of a high-density cementitious rock-maching grout using nano-particles", "Proceedings of ACI Session on "Nanotechnology of Concrete: Recent Developments and Future Perspectives", November 7, Denver, USA (2006), pp. 119-130.

15. Sobolev, K. and Ferrara, M. "How nanotechnology can change the concrete world - Part 2", *American Ceramic Bulletin* (2005), Vol. 84, N°11, pp. 16-20.
16. Sobolev, K. and Ferrara, M. "How nanotechnology can change the concrete world - Part 1", *American Ceramic Bulletin* 84 (10) (2005), pp. 14-17.
17. Sobolev, K., Flores, I. and Hermosillo, R. "Nanomaterials and Nanotechnology for High-performance cement composites, Proceedings of ACI Session on Nanotechnology of Concrete: Recent Developments and Future Perspectives", November 7 (2006), Denver, U.S.A., pp. 91-118.
18. Belkowitz, J.S. and Armentrout, D. "An investigation of nano-silica in the cement hydration process", *Proceeding 2010 Concrete Sustainability Conference*, National Ready Mixed Concrete Association, U.S.A. (2010), pp. 1-15.
19. Quercia, G. and Brouwers, H.J.H. "Application of nano-silica (nS) in concrete mixtures", In Gregor Fisher, Mette Geiker, Ole Hededal, Lisbeth Ottosen, Henrik Stang (Eds.), 8th fib International Ph.D. Symposium in Civil Engineering. Lyngby, June 20-23 (2010), Denmark, pp. 431-436.
20. Rols, S., Ambroise, J. and Péra, J. "Effects of different viscosity agents on the properties of self-leveling concrete", *Cement and Concrete Research* 29 (1999), pp. 261-266.
21. Byung, W.J., Chang, H.K. and Jae, H.L. "Investigations on the Development of Powder Concrete with Nano-SiO₂ Particles", *KSCE Journal of Civil Engineering*, Vol. 11, No. 1 January (2007), pp. 37-42.
22. Collepardi, M., Ogoumah, J.J., Skarp, U. and Troli, R. "Influence of amorphous colloidal silica on the properties of self-compacting concretes", *Proceedings of the International Conference "Challenges in Concrete Construction - Innovations and Developments in Concrete Materials and Construction"*, Dundee, Scotland, UK, 9-11 September (2002), pp. 473-483.
23. Sari, M., Prat, E. and Labastire, J.F. "High strength self-compacting concrete Original solutions associating organic and inorganic admixtures", *Cement and Concrete Research* 29 (1999), pp. 813-818.
24. Sadrumontazi, A. and Barzegar, A. "Assessment of the effect of Nano-SiO₂ on physical and mechanical properties of self-compacting concrete containing rice husk ash", *Proceedings Second International Conference on Sustainable Construction Materials and Technologies*. June 28-30 (2010). Università Politecnica delle Marche, Ancona, Italy, 2010, pp. 1-9.
25. Maghsoudi, A.A. and Arabpour-Dahooei, F. "Effect of nanoscale materials in engineering properties of performance self compacting concrete", *Proceeding of the 7th International Congress on Civil Engineering*. Iran (2007). pp. 1-11.
26. Khanzadi, M., Tadayon, M., Sepehri, H. and Sepehri, M. "Influence of nano-silica particles on mechanical properties and permeability of concrete", *Proceedings Second International Conference on Sustainable Construction Materials and Technologies*. June 28-30 (2010). Università Politecnica delle Marche, Ancona, Italy, 2010, pp. 1-7.
27. Raïess-Ghasemi, A.M., Parhizkar, T. and Ramezani-pour, A.A. "Influence of colloidal nano-SiO₂ addition as silica fume replacement material in properties of concrete", *Proceedings Second International Conference on Sustainable Construction Materials and Technologies*. June 28-30 (2010). Università Politecnica delle Marche, Ancona, Italy, 2010, pp. 1-8.
28. Baomin, W., Lijiu, W. and Lai, F.C. "Freezing resistance of HPC with Nano-SiO₂", *Journal of Wuhan University of Technology, Material Science edition*, Vol.23 No.1, February (2008). Pp. 85-88.
29. Wei, X. and Zhang P. "Sensitivity analysis for durability of high performance concrete containing nanoparticles based on Grey Relational Grade". *Modern Applied Science* Vol. 5, No.4, August (2011), pp. 68-73.
30. Okamura, H. and Ozawa, K. "Mix-design for self-compacting concrete", *Concrete Library, Japanese Society of Civil Engineers- JSCE* Vol. 25 (1995), pp. 107-120.
31. Audenaert, K., Boel, V. and De Schutter, G. "Chloride migration in self compacting concrete", *Proceeding Fifth International Conference on Concrete under Severe Conditions: Environment and Loading (CONSEC'07)*. June 4-6 (2007), Tours, France, pp. 191-298.
32. ENCI B.V. "Betonpocket 2010", Heidelberg Cement Group, 's-Hertogenbosch (2009), The Netherlands (in Dutch), pp. 1-288.
33. Brunauer, S., Emmet, P.H. and Teller, E. "Adsorption of gases in multimolecular layers", *Journal of American Chemical Society* 62 (1938). pp. 309-319.
34. DIN ISO 9277. "Determination of the specific surface area of solids by gas adsorption using the BET method", *German Institute of Normalization-DIN* (2005). pp. 1-19.
35. Hunger, M. "An Integral Design Concept for Ecological Self-Compacting Concrete", Ph.D. Thesis, Eindhoven University of Technology (2010). The Netherlands.
36. Hüsken, G. and Brouwers, H.J.H. "A new mix design concept for earth-moist concrete: A theoretical and experimental study", *Cement and Concrete Research* 38 (2008). pp. 1246-1259.
37. Dutch Normalization-Institute. *Nederlandse invulling van NEN-EN 206-1: Beton Deel 1: Specificatie, eigenschappen, vervaardiging en conformiteit*, Nederlands Normalisatie Instituut, Delft (2008), The Netherlands. pp. 1-72.
38. BMC Certificatie BRL 1801: *Nationale Beoordelingsrichtlijn Betonmortel*. BMC Certificatie, Gouda (2006), The Netherlands (in Dutch).

39. Specification and guidelines for Self Compacting Concrete-SCC, Report, European Federation of Producers and Contractors of Specialist Products for Structures EFNARC. Surrey (2005), UK.
40. BS-EN 12390-2. "Testing hardened concrete - Part 2: Making and curing specimens for strength tests", British Standards Institution-BSI and CEN European Committee for Standardization (2000), pp. 1-10.
41. BS-EN 12390-3. "Testing hardened concrete - Compressive strength of test specimens", British Standards Institution-BSI and CEN European Committee for Standardization (2009), pp. 1-22.
42. BS-EN 12390-6. "Testing hardened concrete - Tensile splitting strength of test specimens", British Standards Institution-BSI and CEN European Committee for Standardization (2000), pp 1-14.
43. Safiuddin, Md. and Hearn, N. "Comparison of ASTM saturation techniques for measuring the permeable porosity of concrete", *Cement and Concrete Research* 35 (2005), pp. 1008-1013.
44. ASTM C1202. "Standard Test Method for Electrical Indication of Concrete's Ability to Resist Chloride Ion Penetration", In *Annual Book of ASTM Standards*, vol. 04.02. American Society for Testing and Materials, Philadelphia, July (2005), pp. 1-6.
45. BS-EN 12390-8. "Testing hardened concrete - Depth of penetration of water under pressure", British Standards Institution-BSI and CEN European Committee for Standardization (2009), pp 1-10.
46. Nordtest method NT Build 492. "Concrete, mortar and cement-based repair materials: Chloride migration coefficient from non-steady-state migration experiments". Finland (1999), pp. 1-8.
47. DuraCrete. "Probabilistic Performance based Durability Design of Concrete Structures", DuraCrete Final Technical Report (2000). Document BE95-1347/R17.
48. CUR Durability Guideline. *Duurzaamheid van constructief beton met betrekking tot chloride-geïnitieerde wapeningscorrosie*. CUR Bouw en Infra. (2009), Gouda, The Netherlands (in Dutch). pp. 1-65.
49. Polder, R.B. "Test methods for on site measurement of resistivity of concrete a RILEM TC-154 technical recommendation", *Construction and Building Materials* 15 (2001), pp. 125-1301.
50. Bentz, D.P., Jensen, O.M., Coats, A.M. and Glasser, F.P. "Influence of silica fume on diffusivity in cement-based materials I. Experimental and computer modeling studies on cement pastes", *Cement and Concrete Research* 30 (2000), pp. 953-962.
51. Nordtest method NT Build 443. "Concrete, hardened: Accelerated chloride penetration". Finland (1995), pp. 1-5.
52. Yuan, Q. "Fundamental studies on test methods for transport of chloride ions in cementitious materials", PhD thesis, Universiteit Gent, Belgium (2009), pp. 1-340.
53. NEN-EN 12390-9. "Testing hardened concrete - Freeze-thaw resistance – Scaling", CEN European Committee for Standardization and Dutch Normalization-Institute, Delft (2006), The Netherlands (in English), pp. 1-29.
54. Korndts, S. and Breit, W. "Combined test method for assessing the workability of SCC-Flow cone", *Concrete Technology Reports* (2004 - 2006), pp. 7-15.
55. Felekoglu, B. "Utilization of high volumes limestone quarry wastes in concrete industry (self-compacting concrete case)", *Resources, Conservation and Recycling* 51 (2007), pp. 770-791.
56. Piechowka-Mielnik, M. and Giergiczny, Z. "Properties of Portland-composite cement with Limestone", *Proceeding of the XIII International Conference on Cement Chemistry, Madrid, July 4-8 (2011)*. pp 1-7.
57. Garboczi, E.J. "Permeability, Diffusivity, and microstructural parameters: A critical review", *Cement and Concrete Research* 20 (1990), pp. 591-601.
58. Yogendran, V. and Langan B.W. "Utilization of silica fume in high strength concrete", In: *Proceedings of utilization of high strength concrete*, Stavanger (1987), Tapir Publisher Trondheim, Norway.
59. Desmet, D., Hernandez, J., Willain, L. and Vantomme, J. "Porosity determination of self-compacting concrete using forced saturation", *Proceeding of the XIII International Conference on Cement Chemistry, Madrid, July 4-8 (2011)*. pp 1-7.
60. Andrade, C., D'Andrea, R., Lopez, J.C., Cienfuegos-Jovellano, A., Alvarez, J.M. and Millan J.M. "Use of electrical resistivity as complementary tool for controlling the concrete production", *Proceeding of the XIII International Conference on Cement Chemistry, Madrid, July 4-8 (2011)*. pp 1-7.
61. Andrade, C., Rio, O., Castillo, A., Castellonte, M. and D' Andrea, R. "A NDT Performance method based on electrical resistivity for the specification of concrete durability", *ECCOMAS Thematic Conference on Computational Methods in Tunneling, Vienna, Austria, August 27-29 (2007)*, pp. 1-9.
62. Romero, H.L., Casati, M.J., Galvez, J.C., Molero, M. and Segura, I. "Study of the damage evolution of concrete under freeze-thaw cycles using traditional and non-traditional techniques", *Proceeding of the XIII International Conference on Cement Chemistry, Madrid, July 4-8 (2011)*. pp 1-7.
63. Neville, A. M. "Properties of Concrete", 4th ed. (2002), Prentice Hall/Pearson, Harlow, U.K. pp. 537-576.
64. Stark, J. and Wicht, B. *Dauerhaftigkeit von Beton: Der Baustoff als Werkstoff*, Birkhäuser, Basel. (2001), Switzerland (in German).
65. Nocun-Wczelik, W. and Loj, G. "Effect of finely dispersed limestone additives of different origin on cement hydration kinetics and cement hardening", *Proceeding of the XIII International Conference on Cement Chemistry, Madrid, July 4-8 (2011)*. pp 1-7.